Field-effect biosensor using virus particles as scaffolds for enzyme immobilization

Arshak Poghossian, Melanie Jablonski, Claudia Koch, Thomas S. Bronder, David Rolka, Christina Wege, Michael J. Schöning

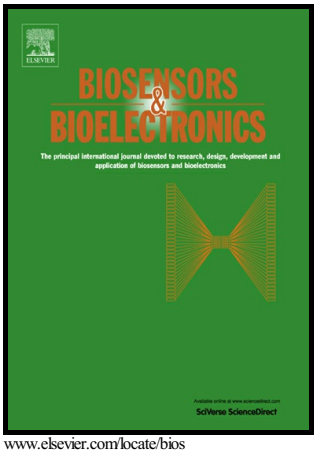

www.elsevier.com/locate/bios

PII: S0956-5663(18)30209-4
DOI: https://doi.org/10.1016/j.bios.2018.03.036
Reference: BIOS10362

To appear in: *Biosensors and Bioelectronic*

Received date: 20 January 2018
Revised date: 1 March 2018
Accepted date: 16 March 2018

Cite this article as: Arshak Poghossian, Melanie Jablonski, Claudia Koch, Thomas S. Bronder, David Rolka, Christina Wege and Michael J. Schöning, Field-effect biosensor using virus particles as scaffolds for enzyme immobilization, *Biosensors and Bioelectronic,* https://doi.org/10.1016/j.bios.2018.03.036

Field-effect biosensor using virus particles as scaffolds for enzyme immobilization

Arshak Poghossian[a,c], Melanie Jablonski[a], Claudia Koch[b], Thomas S. Bronder[a], David Rolka[a,c], Christina Wege[b*], Michael J. Schöning[a,c,*]

[a]Institute of Nano- and Biotechnologies, FH Aachen, Campus Jülich, 52428 Jülich, Germany

[b]Institute of Biomaterials and Biomolecular Systems, University of Stuttgart, 70569 Stuttgart, Germany

[c]Institute of Complex Systems (ICS-8), Forschungszentrum Jülich GmbH, 52425 Jülich, Germany

[*]Corresponding authors: Michael J. Schöning, Tel.: +49-2416-0095-3215;
E-mail address: schoening@fh-aachen.de
Christina Wege, Tel.: +49-711-6856-5073;
E-mail address: christina.wege@bio.uni-stuttgart.de

Abstract

A field-effect biosensor employing *tobacco mosaic virus* (TMV) particles as scaffolds for enzyme immobilization is presented. Nanotubular TMV scaffolds allow a dense immobilization of precisely positioned enzymes with retained activity. To demonstrate feasibility of this new strategy, a penicillin sensor has been developed by coupling a penicillinase with virus particles as a model system. The developed field-effect penicillin biosensor consists of an Al-p-Si-SiO_2-Ta_2O_5-TMV structure and has been electrochemically characterized in buffer solutions containing different concentrations of penicillin G. In addition, the morphology of the biosensor surface with virus particles was characterized by scanning electron microscopy and atomic force microscopy methods. The sensors possessed a high penicillin sensitivity of ~92 mV/dec in a nearly-linear range from 0.1 mM to 10 mM, and a low detection limit of about 50 µM. The long-term stability of the penicillin biosensor was periodically tested over a time period of about one year without any significant loss of sensitivity. The biosensor has also been successfully applied for penicillin detection in bovine milk samples.

Keywords: semiconductor field-effect, *tobacco mosaic virus*, enzyme nanocarrier, penicillinase, penicillin biosensor, milk

1. Introduction

Semiconductor field-effect devices (FED) based on the electrolyte-insulator-semiconductor (EIS) system, like ion-sensitive field-effect transistors, capacitive EIS sensors, light-addressable potentiometric sensors or Si-nanowire transistors, represent one of the most attractive platforms for the development of miniaturized chemical sensors and biosensors (Lee et al., 2009; Molaie, 2016; Nakazato, 2009; Pachauri and Ingebrandt, 2016; Park et al., 2014; Poghossian and Schöning, 2014). These (bio-)chemical sensors are able to directly convert specific biological interactions into electrical signals and have been widely utilized for the detection of pH, concentration of various ions, antibody-antigen affinity binding, biomarkers, DNA hybridization, charged macromolecules, cell acidification, etc. (see e.g., (Bronder et al., 2015; Jimenez-Jorquera et al., 2010; Poghossian et al., 2013; Veigas et al., 2015; Yoshinobu et al., 2017; Zhang and Lieber, 2016). In addition, a large group of enzyme-based FEDs (EnFEDs) have been developed for the detection of different analytes, including, for instance, glucose, urea, penicillin, sucrose, creatinine, adenosine triphosphate, etc. (Beging et al., 2015; Beyer et al., 1994; Dzyadevych et al., 2006; Migita et al., 2007; Poghossian et al., 2015). The most EnFEDs are based on the detection of local pH changes induced by the enzymatic reaction (Beging et al., 2015; Beyer et al., 1994; Dzyadevych et al., 2006). EnFEDs are usually constructed by means of immobilization of a respective enzyme onto the gate surface of the FED. The choice of the appropriate immobilization strategy is essential for the development of biosensors with good performances (high sensitivity, stability, reliability and reusability) and represents one of the most critical points of EnFED construction. The immobilization method should provide a strong attachment of enzymes to the sensor surface, in order to avoid their unwanted detachment during measurements and storage. At the same time, catalytic activity of the enzymes should not be affected to a critical extent upon immobilization to sensor surfaces. Therefore, a broad spectrum of various immobilization methods such as physical adsorption, covalent binding, cross-linking, entrapment within polymeric matrices, mixed physico-chemical methods, etc., has been reported (see e.g., review (Sassolas et al., 2012) for further details). In addition, immobilization techniques based on an incorporation of enzymes on/in nanomaterials have been developed, which aimed to enhance the performance of enzyme biosensors, in particular, EnFEDs (Ansari and Husain, 2012; Siqueira et al., 2010). These techniques include, for example, enzymes embedded within layer-by-layer deposited polyelectrolyte multilayers (Abouzar et al., 2010) or immobilized on top of dendrimer/SWNT (single-walled carbon nanotube) multilayers (Siqueira et al., 2009), enzymes coupled with metal and oxide nanoparticles, (Gun et al.,

2009; Xu et al., 2005) etc. More recently, virus particles have been discussed as a very attractive nanometer-sized scaffolds for the high-density immobilization of biomolecules (in particular, enzymes) and for biosensing (Bäcker et al., 2016; Bruckman et al., 2010; Cardinale et al., 2012; Fan et al., 2015; Mao et al., 2009; Zang et al., 2014; Zang et al., 2017).

Virus particles are precisely defined nanoscale objects that are formed by protein self-assembly (Calo et al., 2016; Fan et al., 2013; Koch et al., 2016). *Tobacco mosaic virus* **(**TMV) was the first plant virus described and is among the best-studied viruses (Koch et al., 2016). TMV infects a wide range of plants (including tobacco, tomato and other members of the family *Solanaceae*), causing characteristic mosaic-like patterns, while it is not capable of inducing diseases in mammals (Calo et al., 2016). TMV is composed of ~2130 identic coat proteins helically self-assembled with a ribonucleic acid genome (Fan et al., 2013; Goelet et al., 1982). This results in a ~300 nm long rigid nanotube with outer and inner channel diameters of 18 nm and 4 nm, respectively (Capek, 2015; Caspar, 1963; Soto and Ratna, 2010). The TMV surface possesses thousands of regularly positioned sites capable for coupling of various (bio-)chemical recognition elements. In addition, by means of modification of the TMV particles with various functional molecules, an enhanced selectivity towards the particular analyte of interest can be achieved (Koch et al., 2015; Lewis et al., 2010). Moreover, it was shown that in comparison to conventional immobilization methods, the binding of enzymes on virus particles can provide an increased enzyme loading and prolonged reusability of sensors (Koch et al., 2015; Koch et al., 2018). Finally, TMV particles functionalized with recognition molecules can be easily integrated with different transducers, thus opening new opportunities for biosensing (Bäcker et al., 2016; Bruckman et al., 2010; Fan et al., 2015; Mao et al., 2009; Zang et al., 2014, Zang et al., 2017).

In this work, we present an EnFED based on a capacitive EIS structure modified with TMV particles as scaffolds for enzyme immobilization. This novel approach for the development of EnFEDs was proposed for the first time by us just recently (Jablonski et al., 2017). As a model system, we use the penicillin/enzyme penicillinase (P) system, because: 1) the detection of penicillin is very important in medicine, fermentation processes, environmental monitoring, food and drug industries; and 2) our many years of expertise with penicillin-sensitive EnFEDs (Abouzar et al., 2010; Beging et al., 2015; Poghossian et al., 2000; Siqueira et al., 2010). The surface morphology of the TMV-modified EIS sensors was characterized by scanning electron microscopy (SEM) and atomic force microscopy (AFM). The developed penicillin biosensor was systematically characterized in buffer solutions

containing different concentrations of penicillin and was applied for the penicillin detection in bovine milk samples for the first time.

2. Materials and methods

2.1. Materials and solutions

The materials, chemicals and solutions used in this work are described in the Supplementary material.

2.2. TMV functionalization

We used genetically modified TMV particles, which expose a cysteine residue (TMV_{Cys}) on each coat protein surface, thus providing thousands of surface thiol groups on the TMV nanotube (Geiger et al., 2013). The enzyme penicillinase was immobilized on the surface of TMV nanotubes by a two-step procedure described in: (Koch et al., 2015; Koch et al., 2018) 1) covalent coupling of biotin linkers (in this study, bifunctional maleimide-PEG_{11}-biotin linkers) to thiol groups of the cysteine residues, resulting in biotinylated TMV particles (TMV_{Cys}/Bio) and 2) bioaffinity binding of streptavidin-penicillinase (SA-P) conjugates to biotin.

Fig. 1 schematically illustrates the biotinylation procedure of TMV_{Cys} particles (a), loading of biotinylated TMV_{Cys}/Bio nanotubes on the EIS sensor surface (b), BSA (bovine serum albumin) blocking (c) and enzyme immobilization via binding of SA-P complexes on the TMV_{Cys}/Bio nanotube surface (d). For biotinylation, TMV_{Cys} were incubated with biotin linker molecules in a molar ratio of 3:1 (linker molecules:coat protein binding sites per TMV nanotube) for 3 h at 30 °C. Afterwards, unbound linker molecules were removed by ultracentrifugation (Beckman Coulter Optima L90K) for 2 h at 18 °C. The TMV_{Cys}/Bio particles were resuspended in 10 mM sodium-potassium-phosphate (SPP) buffer, pH 7. The vast majority of the surface-accessible cysteine residues of TMV_{Cys} particles could be equipped with maleimide-PEG_{11}-biotin linker molecules with a biotinylation efficiency of about 95%, corresponding to approximately 2000 biotin sites per virus particle (Koch et al., 2018). The bifunctional linkers are about 6 nm long and offer increased degrees of freedom for a dense immobilization of SA-P conjugates. The biotinylated TMV_{Cys}/Bio were stored in 10 mM SPP buffer, pH 7. For the details of biotinylation and SA-P conjugation procedures, see (Koch et al., 2018).

Fig. 1

2.3. TMV loading onto the sensor chip and enzyme immobilization

The capacitive field-effect EIS sensors composed of an Al-p-Si-SiO_2-Ta_2O_5 structure with chip sizes of 10 mm × 10 mm were fabricated by standard microfabrication processes. The details of the technological process steps can be found in the Supplementary material. As a pH-sensitive transducer material we use Ta_2O_5, which represents one of the best pH-sensitive materials with a nearly Nernstian pH sensitivity (Beging et al., 2015).

For the loading of TMV nanotubes onto the sensor surface, the chips mounted in measuring chambers were incubated with 70 µl of a 0.1 µg/µl TMV_{Cys}/Bio solution for 1 h at room temperature (RT), followed by washing with polymix buffer (PMB; a detailed description of the PMB composition is given in (Soldatkin et al., 1997)). To prevent/reduce the possible unspecific adsorption of SA-P conjugates on the TMV-free areas of the sensor surface, chips were additionally incubated with PMB containing blocking agents (2% BSA) for 1 h at RT. Thereafter, the SA-P complexes were immobilized on the TMV_{Cys}/Bio nanotubes by means of biotin-SA affinity binding that allows control over the orientation of biomolecules (Chen et al., 2013; Koch et al., 2015). In this way, full preservation of enzyme activity after the immobilization of streptavidin-conjugated enzymes on biotinylated TMV nanotubes can be achieved as it has been reported in (Koch et al., 2015; Koch et al., 2018). An immobilization of SA-P conjugates was realized by incubation of 70 µl SA-P solution (11.8 µg or 30 Units) on the EIS sensor surface for 2 h at RT in a humid chamber.

2.4. Functioning of the capacitive field-effect penicillin biosensor and measurement setup

The penicillin biosensor developed in this work is built-up of a pH-sensitive Ta_2O_5-gate EIS structure modified with TMV nanotubes functionalized with SA-P conjugates. Fig. 2 schematically shows the TMV-modified EIS sensor mounted in a measuring chamber and sealed with an O-ring, the measurement setup and the enzymatic reaction of a penicillinase-catalyzed hydrolysis of penicillin. The operation principle of the field-effect penicillin biosensor based on a capacitive EIS structure is described in our previous works (see e.g., (Abouzar et al., 2010; Beging et al., 2015)). Briefly, the EIS sensor detects changes in the concentration of hydrogen ions near the surface of the pH-sensitive gate insulator (in this study, Ta_2O_5) induced due to the hydrolysis of the β-lactam ring of the penicillin specifically catalyzed by the enzyme P. The resulting local pH decrease will alter the surface charge of the Ta_2O_5 layer and the depletion capacitance in the silicon and thus, will lead to penicillin concentration-dependent changes in the overall capacitance of the EIS biosensor. Hence, the

penicillin concentration in the test solution can quantitatively be determined using the calibration curve of the EIS biosensor.

Fig. 2

The unmodified (bare) and TMV-modified EIS sensors were electrochemically characterized by means of capacitance-voltage (*C–V*) and constant-capacitance (ConCap) methods using an impedance analyzer (Zahner Zennium, Zahner Elektrik, Germany). In addition, the leakage current of bare sensors has been proven to verify quality of the gate insulator. The contact area of the sensor surface with solution was defined by the inner diameter of the O-ring and amounted ~0.5 cm^2. To achieve a lower detection limit and a higher sensitivity, penicillin measurements were performed in a low-capacity working buffer (in this study, 0.25 mM PMB containing 100 mM KCl as ionic-strength adjuster, pH 8).

For the *C−V* measurements, a DC (direct current) gate voltage (V_G) ranging from −4 V to +2 V was applied between the reference electrode and the rear-side Al contact. An additional small AC (alternating current) voltage (20 mV) with a frequency of 120 Hz was superimposed in order to measure the capacitance of the EIS structure at different gate voltages. During the ConCap measurements, the capacitance of the EIS sensor at the working point was kept constant, and the penicillin concentration-dependent potential changes at the Ta_2O_5-gate surface (due to the local pH changes induced by the enzymatic reaction) were recorded directly. The working point (i.e., constant-capacitance value) for the ConCap-mode measurements was chosen within the depletion region of the recorded *C−V* curve (for details of *C−V* and ConCap modes, see e.g. (Poghossian et al., 2013)). A conventional Ag/AgCl liquid-junction electrode (3 M KCl, Metrohm, Germany) was used as a reference electrode.

Before starting the experiments, the pH value of all solutions was measured with a commercial pH-glass electrode (Mettler Toledo, Germany). All measurements were carried out at RT and in a dark Faraday cage (in order to reduce the possible impact of ambient light and electromagnetic fields on a sensor response). When not in use, the biosensors installed in the measurement chambers were stored in PMB at 4 °C.

3. Results and discussion

3.1. Leakage current and C-V curve of the bare EIS chips

The leakage-current level and the shape of the *C–V* curve are crucial factors for a correct functioning of the EIS sensors and therefore, were checked before TMV loading onto the

chips. The leakage current is often used to characterize the quality of the gate oxide (in this study, a double layer of SiO_2-Ta_2O_5) and should be very small. The leakage current was measured in PMB at applied gate voltages (between the reference electrode and rear-side Al contact of the EIS chip) ranging from −3 V to +3 V. Only chips having a maximum leakage current less than 10 nA were selected for further TMV-loading and penicillin-detection experiments.

The potential sensitivity of the EIS structures was tested via *C–V* measurements. Fig. 3a shows a typical high-frequency *C–V* curve of the bare EIS sensor measured in PMB. The *C–V* curve has a usual p-type behavior with a characteristic sigmoidal-like shape and typical accumulation (V_G< −2 V), depletion (−2 V < V_G< −0.2 V) and inversion (V_G> −0.2 V) regions. The maximum capacitance in the accumulation region, where the total capacitance is determined by the capacitance of the gate insulator, was 49.5±1.5 nF. This value correlates well with the calculated geometrical capacitance for a double-layer gate insulator consisting of 30 nm SiO_2 and 60 nm Ta_2O_5.

The *C-V* curve is slightly deformed in the depletion region that is usually due to the existence of a series resistance (in this work, resistance of the reference electrode). As it has been demonstrated in (Demoz et al., 1995; Estrada del Cueto and Altuzarra, 1996; Mourzina et al., 2003; Poghossian et al., 2004), any resistance in series with an EIS capacitance (e.g., impedance of the reference electrode, resistance of low-ionic-strength electrolyte solution, resistances of Si substrate and back-side contact) could lead to a deformation of the experimental *C–V* curves of the EIS structures. However, this effect has no impact on the basic results obtained in this work, because the ConCap characterization of sensors was performed at constant-capacitance values chosen from the linear range of the depletion region.

3.2. pH sensitivity of the bare and TMV-modified EIS sensors

Since the operating principle of penicillin-sensitive EnFEDs is based on the local pH decrease induced due to the enzymatic hydrolysis of penicillin, the pH sensitivity of bare and TMV-modified Ta_2O_5-gate EIS sensors was proven. Fig. 3b shows an example of ConCap signal of a bare and a TMV-modified EIS sensor measured in Titrisol buffer solutions (Merck, Germany) with various pH values between pH 6 and pH 9. The mean pH sensitivity of the unmodified EIS sensor with Ta_2O_5 layer was about 58 mV/pH, which conforms to values previously reported for Ta_2O_5 layers (see e.g., (Beging et al., 2015; Cane et al., 1997)). A

slightly smaller pH sensitivity of 55 mV/pH was observed for EIS sensors modified with TMV nanotubes with immobilized enzyme P.

Fig. 3

3.3. SEM and AFM characterization of EIS-chip surface modified with TMV particles

The EIS chips were characterized by SEM and AFM methods to gain a picture of how the morphology of the Ta_2O_5 surface changed after loading of the TMV nanotubes. SEM images have been collected using a Jeol JSM-7800F (Fa. JEOL GmbH, Germany). Tapping-mode AFM images were taken in air using a BioMAT Workstation (JPK Instruments, Germany) and silicon cantilevers with tip radii <10 nm (NanoWorld AG, Switzerland).

Fig. 4 represents an example of an SEM image (a) and a tapping-mode AFM height profile (b) of the EIS-sensor surface modified with TMV nanotubes. Single TMV nanotubes can clearly be recognized in the SEM and AFM images. In addition, shortened TMV particles of about 100-200 nm length can be seen. The mean surface density of TMV nanotubes, evaluated from several SEM images, was approximately 2×10^9 TMV/cm^2 or 1×10^9 TMV nanotubes per sensor with an active sensing area of 0.5 cm^2. As described in Section 2.2., most surface cysteine residues of TMV_{Cys} particles could be equipped with maleimide-PEG_{11}-biotin linker molecules with a biotinylation efficiency of about 95% of the 2130 coat protein subunits (Koch et al., 2018), resulting in approximately 2000 biotin sites per virus nanotube. The coupling efficiency of SA-enzyme conjugates to biotin sites displayed on TMV nanotubes is typically about 100% (Koch, et al. 2015). Taking into account that the part of the surface biotin moieties (~20% of all biotin molecules per virus nanotube) were not accessible for enzyme immobilization as they were facing towards the sensor surface, the estimated density of enzyme P molecules amounted to approximately 3.2×10^{12} enzymes/cm^2 or 1.6×10^{12} enzyme molecules per sensor.

Fig. 4

3.4. Penicillin detection with TMV-modified EIS sensors

Four TMV-modified EIS biosensors were characterized in PMB with different concentrations of penicillin G ranging from 20 µM to 20 mM. To test the long-term behaviour, the biosensors were periodically tested over a time period of about 1 year. During this time period, each biosensor was used for more than 70 penicillin measurements. After

each measurement in penicillin solution, the sensor surface was rinsed several times. As an example, Fig. 5a demonstrates the dynamic ConCap signal of a TMV-modified EIS penicillin biosensor (Sensor 1) recorded on the 15th day after enzyme immobilization. The measurement cycle starts with ConCap measurement in working buffer.

Fig. 5

As can be seen, the measured ConCap signal shows a clear dependence on the penicillin concentration. As discussed in Section 2.4, the local pH decrease on/nearly to the sensor surface (resulting from the enzymatic hydrolysis of penicillin) will alter the gate-surface charge and thus, will lead to penicillin concentration-dependent changes in the total capacitance of the EIS biosensor. As a consequence, with increasing penicillin concentration, the ConCap-mode response of the field-effect biosensor is shifted in the direction of more negative voltages (a similar behavior was observed for all four sensors). For example, the potential shift of ~185 mV has been recorded for Sensor 1 at a penicillin concentration of 10 mM. Taking into account the pH-sensitivity value of 55 mV/pH for TMV-modified EIS sensors, the potential change of 185 mV corresponds to a local pH decrease of about ΔpH≈3.36. From the ConCap curve in Fig. 5a, the penicillin sensitivity of ~98 mV/dec was calculated for the quasi-linear concentration range of 0.1 – 10 mM penicillin. The hysteresis of the sensor signal at a penicillin concentration of 5 mM amounted to about 4 mV. The estimated lower detection limit was around 50 µM, although some sensors were able to detect even penicillin concentrations as low as 20 µM (see Fig. 5a). To demonstrate long-term stability of TMV-modified EIS sensors, Fig. 5b shows the ConCap curves for Sensor 1 and Sensor 2 measured on the 297th and 355th day after enzyme immobilization, respectively. Even after such a long operation and storage period, penicillin sensors with TMV nanotubes as enzyme nanocarriers showed a clear dependence on the penicillin concentration, a significant sensor response even at low concentrations and a high sensitivity. These striking results obtained for the long-term stability of all four sensors are summarized in Fig. 5c in form of a vertical-bar diagram. When stored in a 0.25 mM PMB at 4 °C and periodically measured in penicillin solutions with different concentrations, the EIS penicillin biosensors were stable for at least ~1 year with sensitivity-value's fluctuation within not more than ±6 mV/dec at a mean penicillin sensitivity of about 92 mV/dec.

The obtained values for the penicillin sensitivity of TMV-modified EIS sensors were higher than reported in (Baur et al., 2006; Beging et al., 2015; Liu et al., 1998) (for instance,

penicillin sensitivity of ~47 mV/dec was reported for the EIS-penicillin biosensor with adsorptively immobilized penicillinase (Beging et al., 2015)) and comparable or a little bit lower to those that have been discussed in (Abouzar et al., 2010; Beyer et al., 1994). Nevertheless, because of different gate insulators, enzyme-immobilization techniques, enzyme activity, buffer solutions used, a direct comparison of basic parameters of the penicillin biosensor developed in this work with those reported previously is difficult.

3.5. Penicillin detection in milk

The detection and quantification of penicillin is very important in clinical laboratories, drug (e.g., antibiotic tablets and injectables) and food (e.g., milk, meat) quality control, for environmental monitoring and process control in biotechnology. In dairy farming, antibiotics are used not only for the treatment of food-producing animals, but also for infection prophylaxis and as feed supplement in order to promote growth and improve livestock-production efficiency in some countries (Graham et al., 2007). This can lead to human health problems due to the transfer of antibiotic residues into the food (e.g., meat, milk, eggs). Moreover, the wide application of antibiotics in human medicine and treatment of food-producing animals contributes to the alarming spread of antibiotic-resistant bacteria. Due to their low cost, simplicity and possibility for rapid real-time analysis, the application of field-effect EIS biosensors for the detection of antibiotic residues is a good alternative to traditional methods.

In this study, in proof-of-principle experiments, the TMV-modified EIS biosensor has been applied for the detection of penicillin in milk (long-life 1.5% fat bovine milk). Fig. 6a exemplarily shows a ConCap signal of the TMV-modified EIS biosensor recorded in PMB and milk-buffer mixtures of pH 6.8 and pH 8, respectively, without penicillin or spiked with 5 mM penicillin.

Fig. 6

The pH value of milk measured with a conventional pH-glass electrode was about pH 6.8. Therefore, experiments were started by measurement of the ConCap signal of the TMV-modified EIS sensor in PMB of pH 6.8. An addition of 5 mM penicillin G in buffer resulted in a potential shift of about 122 mV. This value is smaller than that recorded in PMB of pH 8 containing 5 mM penicillin (172 mV in Fig. 5 and 163 mV in Fig. 6a), probably due to a suboptimal pH working range for the enzyme penicillinase (the optimal pH for penicillinase

activity was reported to be pH 8) (Sawai et al., 1976). The addition of 5 mM penicillin G in a milk sample of pH 6.8 induced a signal change of 17 mV only (~7 times smaller than the potential shift observed in a low-capacity 0.25 mM PMB, pH 6.8), because milk possesses a strong buffering effect. Therefore, in order to enhance the sensor performance, in further experiments, the penicillin biosensor was tested in milk samples diluted in a low-capacity buffer (milk:PMB mixture of 1:10) of pH 6.8 and pH 8, supplemented with 5 mM penicillin G. As expected, decreasing the pH-buffering capacity of milk samples (pH 6.8) via dilution resulted in an enhanced sensor signal of about 74 mV. However, the higher sensor signal of about 106 mV was observed in a milk-buffer mixture at the optimal pH for penicillinase activity of pH 8.

Finally, the TMV-modified EIS biosensor was tested in a milk-buffer mixture spiked with different concentrations of penicillin from 10 µM to 1 mM (see Fig. 6b). The penicillin sensitivity of the EIS biosensors tested in milk-buffer samples was about 32 mV/dec in the range from 50 µM to 1 mM penicillin. The biosensor depicts a distinct signal change of 5 mV even at a low penicillin concentration of 50 µM in milk. The penicillin sensitivity of the biosensor in milk was smaller than that in buffer solution, which can be attributed to the complex composition of milk and the possible binding of penicillin molecules to milk proteins (Grunwald and Petz, 2003). The presence of milk proteins may also affect the sensor signal due to the possible non-specific adsorption of proteins on the biosensor surface. Nevertheless, the novel TMV-modified field-effect biosensor demonstrated its functionality, even in such complex matrices.

4. Conclusions

At present, viruses are considered not only as agents that cause various diseases, but also as very attractive nanoscale building blocks for many fields of applications, including biosensorics, nano- and biotechnology. In this study, a capacitive field-effect biosensor modified with TMV nanotubes as scaffolds for the dense immobilization of enzymes has been realized using penicillin/penicillinase as model system. The developed penicillin biosensors consisting of an Al-p-Si-SiO_2-Ta_2O_5-TMV structure have been characterized in penicillin G solutions of different concentrations in terms of sensitivity, linear range, detection limit and long-term stability. The biosensors possessed a high penicillin sensitivity of about 92 ± 6 mV/dec, a low detection limit of about 50 µM and a remarkable long-term stability. Even after one year of repeated testing, the sensor performance was fully preserved. Furthermore, proof-of-principle experiments demonstrated the suitability of the developed biosensor for the

penicillin detection in diluted milk samples. To our knowledge, this is the first use of virus particles as enzyme nanocarriers for a field-effect detection of antibiotics in milk. However, the lower detection limit of our penicillin biosensor is beyond the maximum residue limit stated by the European Union regulations for penicillin G (benzylpenicillin) in milk (4 μg/kg or 12 nM) and all food-producing species (50 μg/kg or 150 nM) (see e.g., Babington et al., 2012), and therefore, should be improved. At the same time, the detection limit and operating range of the TMV-modified EIS penicillin biosensor achieved in this study matches the typical application range in biotechnology, in particular, for the control of penicillin G content in fermentation broth during biotechnological production of benzylpenicillin.

Although in the present study, the immobilization of the enzyme penicillinase on TMV nanotubes was used as a model system for penicillin measurements, most likely, this novel concept could be adapted to other enzymes and biomolecules. The results obtained in this work demonstrate a great potential of an integration of virus/biomolecule hybrids with electronic transducers, thereby opening new opportunities in advanced label-free biosensing technology. Future experiments will be directed to test field-effect biosensors modified with TMV nanotubes carrying several different enzymes, thus enabling a simultaneous detection of multiple analytes.

Declarations of interest: The authors declare no competing financial interest.

Acknowledgements

The authors thank H. Iken for the fabrication of EIS chips, J. Arreola for the AFM images, D. Gotthardt and M. Mueller for taking good care of the tobacco plants and H. Jeske for valuable discussions.

Appendix A. Supplementary material

Supplementary data associated with this article can be found in the online version.

References

Abouzar, M.H., Poghossian, A., Siqueira Jr J.R., Oliveira Jr, O.N., Moritz, W., Schöning, M.J., 2010. Phys. Status Solidi A 207, 884–890.

Ansari, S.A., Husain, Q., 2012. Biotechnol. Adv. 30, 512–523.

Babington, R., Matas, S., Marco, M.-P., Galve, R., 2012. Anal. Bioanal. Chem. 403, 1549–1566.

Bäcker, M., Koch, C., Eiben, S., Geiger, F., Eber, F., Gliemann, H., Poghossian, A., Wege, C., Schöning, M.J., 2016. Sens. Actuators B 238, 716–722.

Baur, B., Howgate, J., von Ribbeck, H.-G., Gawlina, Y., Bandalo, V., Steinhoff, G., Stutzmann, M., Eickhoff, M., 2006. Appl. Phys. Lett. 89, 183901.

Beging, S., Leinhos, M., Jablonski, M., Poghossian, A., Schöning, M.J., 2015. Phys. Status Solidi A 212, 1353–1358.

Beyer, M., Menzel, C., Quack, R., Scheper, T., Schügerl, K., Treichel, W., Voigt, H., Ullrich, M., Ferretti, R., 1994. Biosens. Bioelectron. 9, 17–21.

Bronder, T.S., Poghossian, A., Scheja, S., Wu, C., Keusgen, M., Mewes, D., Schöning, M.J., 2015. ACS Appl. Mater. Interfaces 7, 20068–20075.

Bruckman, M.A., Liu, J., Koley, G., Li, Y., Benicewicz, B., Niu, Z., Wang, Q., 2010. J. Mater. Chem. 20, 5715–5719.

Calo, A., Eiben, S., Okuda, M., Bittner, A.M., 2016. Jpn. J. Appl. Phys. 55, 03DA01.

Cane, C., Gracia, I., Merlos, A., 1997. Microelectron. J. 28, 389−405.

Capek, I., 2015. Adv. Colloid Interface Sci. 222, 119–134.

Cardinale, D., Carette, N., Michon, T., 2012. Trends Biotechnol. 30, 369–376.

Caspar, D.L., 1963. Adv. Protein Chem. 18, 37–121.

Chen, C., Xie, Q., Yang, D., Xiao, H., Fu, Y., Tan, Y., Yao, S., 2013. RSC Adv. 3, 4473–4491.

Demoz, A., Verpoorte, E.M.J., D.J. Harrison, D.J., 1995. J. Electroanal. Chem. 389, 71–78.

Dzyadevych, S.V., Soldatkin, A.P., El'skaya, A.V., Martelet, C., Jaffrezic-Renault, N., 2006. Anal. Chim. Acta 568, 248–258.

Estrada del Cueto, M., Altuzarra, A.C., 1996. Solid-State Electron. 39, 1519–1521.

Fan, X.Z., Pomerantseva, E., Gnerlich, M., Brown, A., Gerasopoulos, K., McCarthy, M., Culver, J., Ghodssi, R., 2013. Vac. Sci. Technol. A 31, 050815.

Fan, X.Z., Naves, L., Siwak, N.P., Brown, A., Culver, J., Ghodssi, R., 2015. Nanotechnology 26, 205501.

Geiger, F.C., Eber, F.J., Eiben, S., Mueller, A., Jeske, H., Spatz, J.P., Wege, C., 2013. Nanoscale 5, 3808–3816.

Goelet, P., Lomonossoff, G.P., Butler, P.J., Akam, M.E., Gait, M.J., Karn, J.,1982. Proc. Nat. Acad. Sci. USA 79, 5818–5822.

Graham, J. P., Boland, J.J., Silbergeld, E., 2007. Public Health Rep. 122, 79–87.

Grunwald, L., Petz, M., 2003. Anal. Chim. Acta 483, 73–79.

Gun, J., Rizkov, D., Lev, O., Abouzar, M.H., Poghossian, A., Schöning, M.J., 2009. Microchim. Acta 164, 395–400.

Jablonski, M., Koch, C., Bronder, T. S., Poghossian, A., Wege, C., Schöning, M. J., 2017. Proceedings 1, Article 505.

Jimenez-Jorquera, C., Orozco, J., Baldi, A., 2010. Sensors 10, 61–83.

Koch, C., Wabbel, K., Eber, F.J., Krolla-Sidenstein, P., Azucena, C., Gliemann, H., Eiben, S., Geiger, F., Wege, C., 2015. Front. Plant Sci. 6, Article 1137.

Koch, C., Eber, F.J., Azucena, C., Förste, A., Walheim, S., Schimmel, T., Bittner, A.M., Jeske, H., Gliemann, H., Eiben, S., Geiger, F.C., Wege, C., 2016. Beilstein J. Nanotechnol. 7, 613–629.

Koch, C., Poghossian, A., Schöning, M.J., Wege, C., 2018. Nanotheranostics, 2, 184–196.

Lee, C.S.; Kim, S.K.; Kim, M., 2009. Sensors 9, 7111–7131.

Lewis, C.L., Lin, Y., Yang, C., Manocchi, A.K., Yuet, K.P., Doyle, P.S., Yi, H., 2010. Langmuir 26, 13436–13441.

Liu, J., Liang, L., Li, G., Han, R., Chen, K., 1998. Biosens. Bioelectron. 13, 1023–1028.

Mao, C., Liu, A., Cao, B., 2009. Angew. Chem. Int. Ed. 48, 6790–6810.

Migita, S., Ozasa, K., Tanaka, T., Haruyama, T., 2007. Anal. Sci. 23, 45–48.

Molaie, M., 2016. Nanomed. J. 3, 69–82.

Mourzina, Yu., Mai, Th., Poghossian, A., Ermolenko, Yu., Yoshinobu, T., Vlasov, Yu., Iwasaki, H., Schöning, M.J., 2003. Electrochim. Acta 48, 3333–3339.

Nakazato, K., 2009. Sensors 9, 8831–8851.

Park, J., Nguyen, H.H., Woubit, A., Kim, M., 2014. Appl. Sci. Convergence Technol. 23, 61–71.

Pachauri, V., Ingebrandt, S., 2016. Essays Biochem. 60, 81–90.

Poghossian, A., Thust, M., Schöning M.J., Müller-Veggian, M., Kordos, P., Lüth, H., 2000. Sens. Actuators B 68, 260–265.

Poghossian, A., Mai, D.-T., Mourzina, Yu., Schöning, M.J., 2004. Sens. Actuators B 103, 423–428.

Poghossian, A., Weil, M., Cherstvy, A.G., Schöning, M.J., 2013. Anal. Bioanal. Chem. 405, 6425–6436.

Poghossian, A., Schöning, M.J., 2014. Electroanalysis 26, 1197–1213.

Poghossian, A., Katz, E., Schöning, M.J., 2015. Chem. Commun.51, 6564–6567.

Sassolas, A., Blum, L.J., Leca-Bouvier, B.D., 2012. Biotechnol. Adv. 30, 489–511.

Sawai, T., Morioka, K., Ogawa, M., Yamagishi, S., 1976. Antimicrob. Agents Chemother. 10, 191–195.

Siqueira, J., Maki, R.M., Paulovich, F.V., Werner, C.F., Poghossian, A., de Oliveira, C.F., Zucolotto, V., Oliveira Jr., O.N., Schöning, M.J., 2010. Anal. Chem. 82, 61–65.

Siqueira Jr, J.R., Abouzar, M.H., Bäcker, M., Zucolotto, V., Poghossian A., Oliveira Jr, O.N., Schöning, M.J., 2009. Phys. Status Solidi A 206, 462–467.

Siqueira Jr, J.R., Caseli, L., Crespilho, F.N., Zucolotto, V., Oliveira Jr, O.N., 2010. Biosens. Bioelectron. 25, 1254–1263.

Soldatkin, A.P., Gorchkov, D.V., Martelet, C., Jaffrezic-Renault, N., 1997. Mater. Sci. Eng. C 5, 35–40.

Soto, C.M., Ratna, B.R., 2010. Curr. Opin. Biotechnol. 21, 426–438.

Veigas, B., Fortunato, E., Baptista, P.V., 2015. Sensors 15, 10380–10398.

Xu, J.J., Zhao, W., Luo, X.L., Chen, H.Y., 2005. Chem. Commun. 6, 792–794.

Yoshinobu, T., Miyamoto, K., Werner, C.F., Poghossian, A., Wagner, T., Schöning, M.J., 2017. Annu. Rev. Anal. Chem. 10, 225–246.

Zang, F., Gerasopoulos, K., Fan, X.Z., Brown, A.D., Culver, J.N., Ghodssi, R., 2014. Chem. Commun. 50, 12977–12980.

Zang, F., Gerasopoulos, K., Brown, A.D., Culver, J.N., Ghodssi, R., 2017. ACS Appl. Mater. Interfaces 9, 8471–8479.

Zhang, A., Lieber, C.M., 2016. Chem. Rev. 116, 215–257.

Figure captions

Fig. 1. Biotinylation of TMV_{Cys} particles (a), loading of biotinylated TMV_{Cys}/Bio nanotubes onto the EIS sensor surface (b), BSA blocking (c) and enzyme immobilization via binding of SA-P complexes on the TMV_{Cys}/Bio nanotube surface (d) (schematically).

Fig. 2. Schematic structure of TMV-modified capacitive EIS biosensor mounted in the measuring chamber, measurement setup as well as enzymatic reaction of penicillin hydrolysis catalyzed by the enzyme P.

Fig. 3. *C–V* curve of bare Ta_2O_5-gate EIS sensor (a) as well as ConCap signal of EIS sensor before and after modification with TMV particles measured in Titrisol buffer solutions with different pH values (b). The working point (constant-capacitance value of 25 nF) for ConCap measurements was chosen within the linear range of the depletion region of the recorded *C–V* curve.

Fig. 4. SEM image (a) and AFM height profile (b) of the EIS sensor surface modified with TMV nanotubes. Scanned area: $2 \times 2\ \mu m^2$.

Fig. 5. a) ConCap signal of a TMV-modified EIS-penicillin biosensor (Sensor 1) measured in PMB containing different concentrations of penicillin ranging from 20 µM to 20 mM on the 15^{th} day after enzyme immobilization. b) ConCap curves for Sensor 1 and Sensor 2 measured on 297^{th} and 355^{th} day after enzyme immobilization, respectively. c) Bar chart of the long-term sensitivity of penicillin biosensors.

Fig. 6. a) ConCap response of TMV-modified EIS sensor measured in PMB (polymix buffer) and milk-buffer mixture of pH 6.8 and pH 8 without penicillin or spiked with 5 mM penicillin; b) ConCap response recorded in milk-buffer mixture containing different concentrations of penicillin ranging from 10 µM to 1 mM.

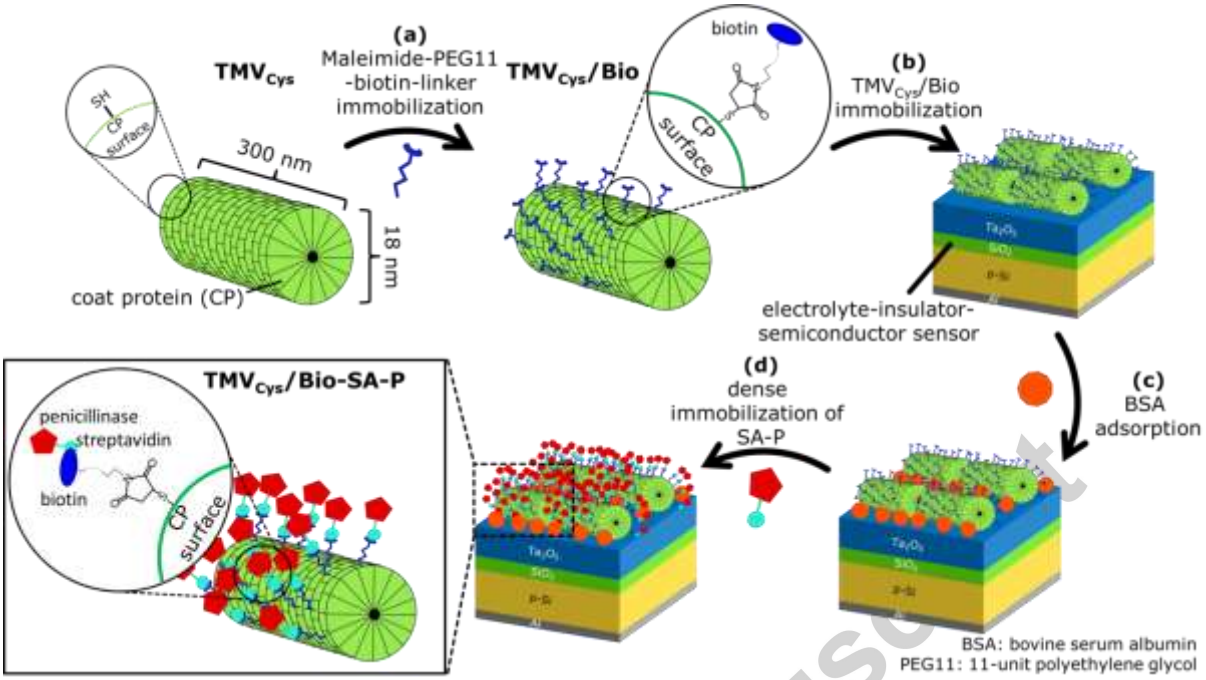

Fig. 1

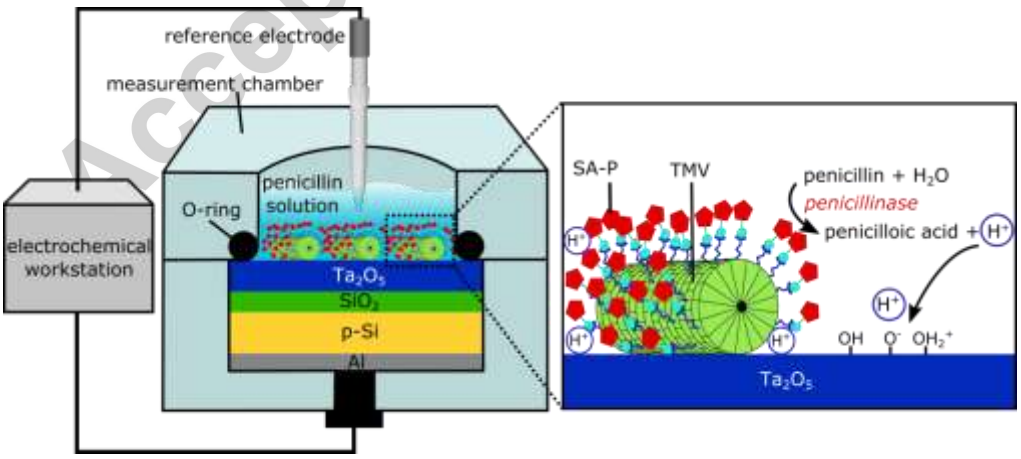

Fig. 2

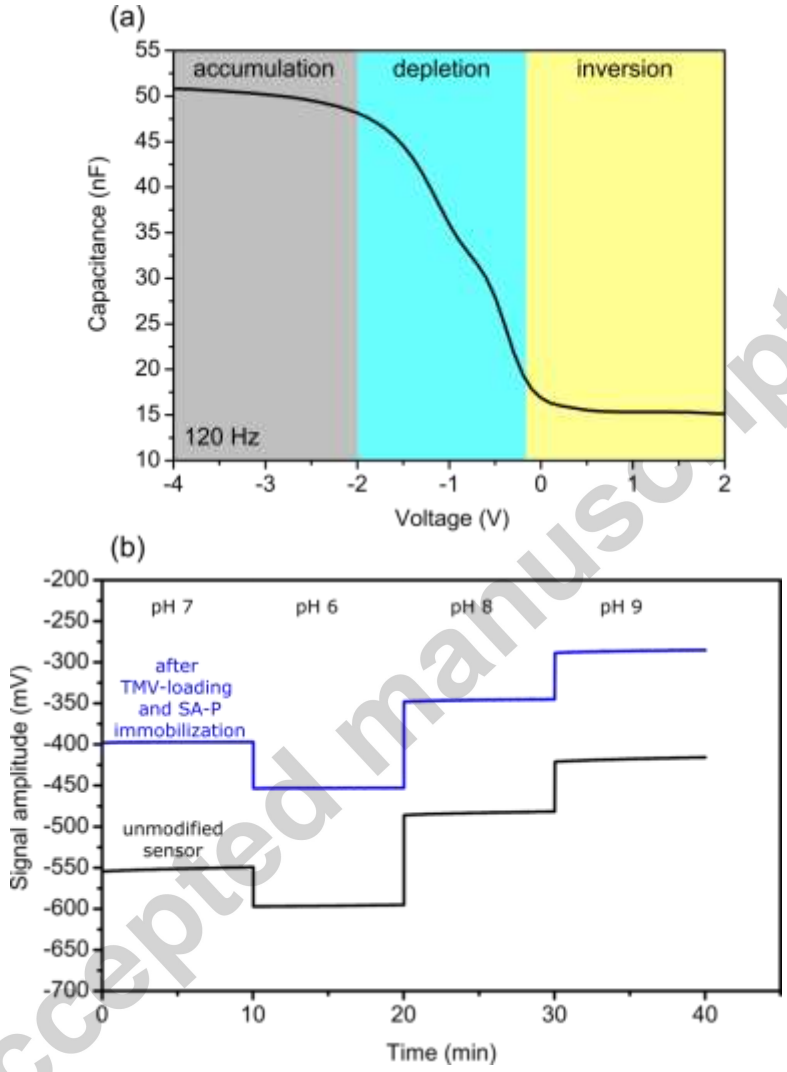

Fig. 3

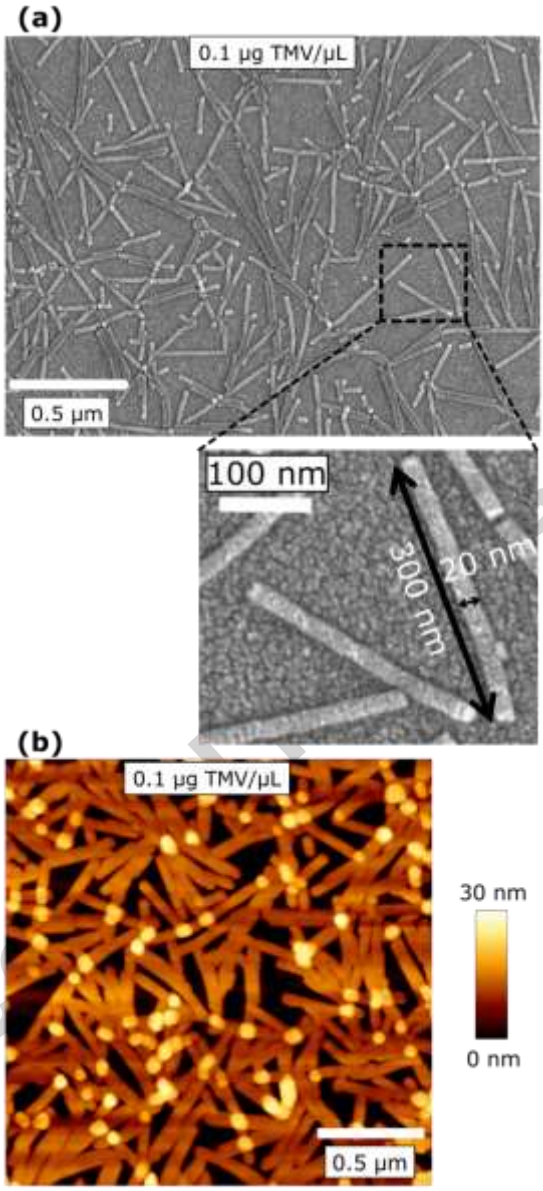

Fig. 4

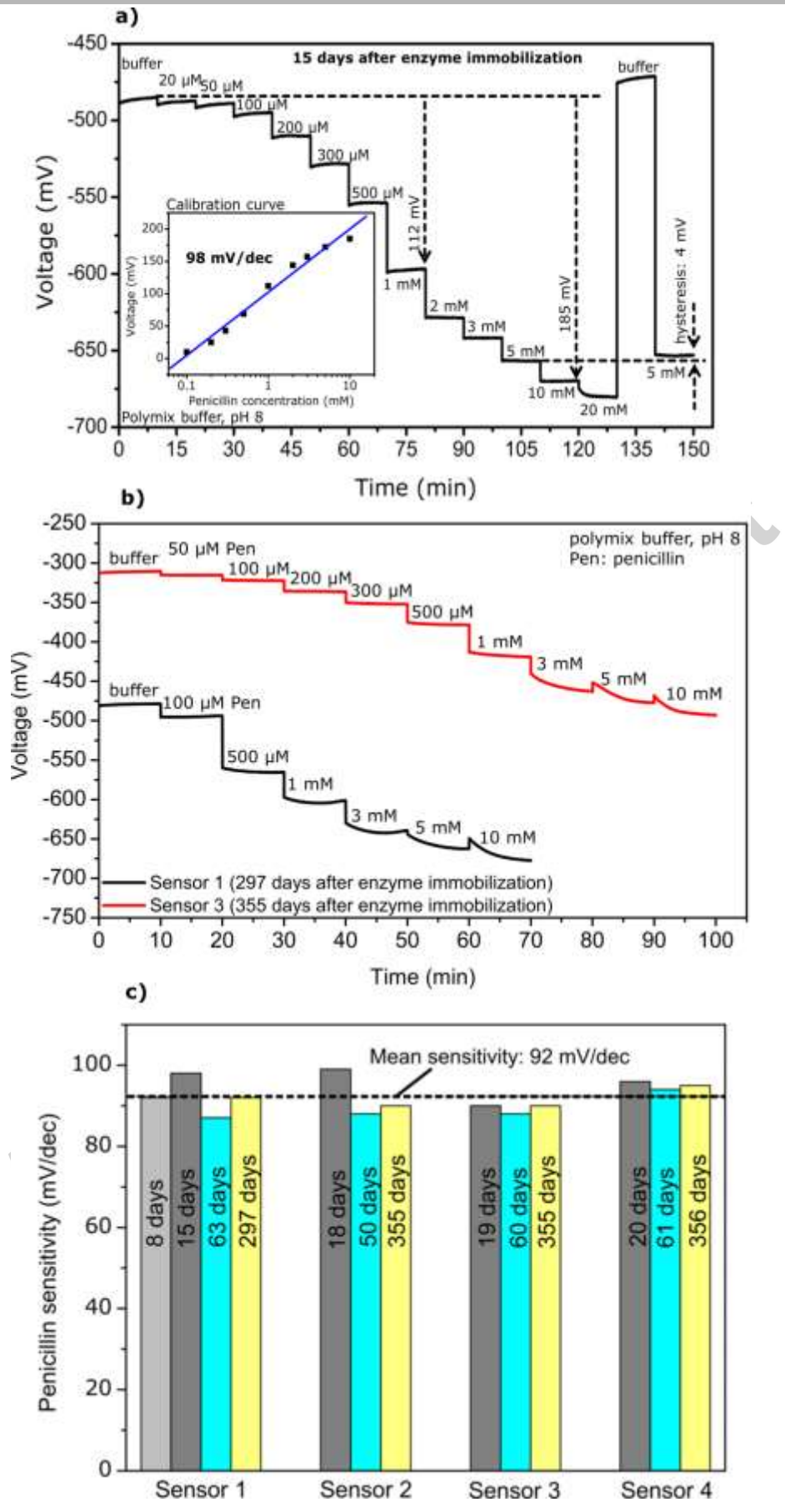

Fig. 5

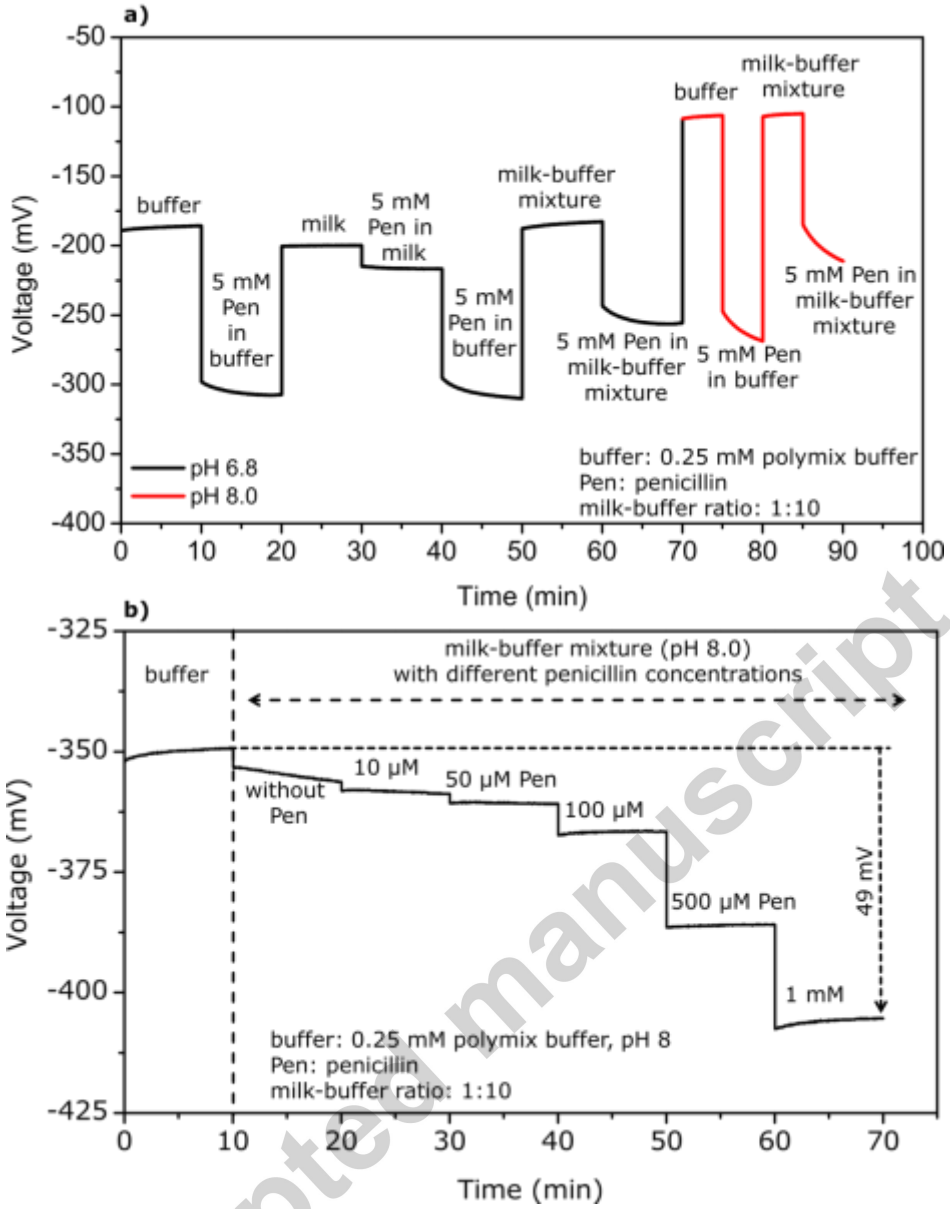

Fig. 6

Highlights

- A field-effect biosensor modified with *tobacco mosaic virus* (TMV) nanotubes as enzyme nanocarrier is presented.
- TMVs applied as adapter scaffolds enable a dense immobilization of precisely positioned enzymes with retained activity.
- Based on this new strategy, a penicillin biosensor was developed by coupling the enzyme penicillinase with virus particles loaded onto the sensor chip.
- The biosensor was successfully applied for penicillin detection in bovine milk samples.